Human Molecular Genetics, 2016, Vol. 25, No. 12 2539–2551

doi: 10.1093/hmg/ddw117
Advance Access Publication Date: 3 June 2016
Original Article

ORIGINAL ARTICLE

Increased steroidogenesis promotes early-onset and severe vision loss in females with *OPA1* dominant optic atrophy

Emmanuelle Sarzi[1,*], Marie Seveno[1], Claire Angebault[1], Dan Milea[2,3,4,5], Cecilia Rönnbäck[6,7], Melanie Quilès[1,8], Mathias Adrian[1], Joanna Grenier[1,9], Angélique Caignard[2], Annie Lacroux[1,9], Christian Lavergne[10], Pascal Reynier[2], Michael Larsen[6,7], Christian P. Hamel[1,9], Cécile Delettre[1], Guy Lenaers[1,11,†] and Agnès Müller[1,8,†]

[1]INSERM U1051 – Institut des Neurosciences de Montpellier, Montpellier, France, [2]Département de Biochimie et Génétique, UMR CNRS 6214-INSERM 1083, Centre Hospitalier Universitaire, Angers, France, [3]Singapore National Eye Centre, Singapore, [4]Singapore Eye Research Institute, Singapore, [5]Duke-NUS, Singapore, [6]Department of Ophthalmology, Glostrup Hospital, Glostrup, Denmark, [7]Faculty of Health and Medical Sciences, University of Copenhagen, Copenhagen, Denmark, [8]Université de Montpellier - Faculté de Pharmacie-Montpellier, France, [9]Centre de référence des affections sensorielles d'origine génétique, Hôpital Gui de Chauliac, Montpellier, France, [10]Institut Montpelliérain Alexander Grothendieck. Université Montpellier 3, France and [11]PREMMI, UMR CNRS 6214-INSERM 1083, Université d'Angers, France

*To whom correspondence should be addressed at Institut des Neurosciences de Montpellier, Hôpital St Eloi, 34091 Montpellier, France, e-mail: emmanuelle.sarzi@inserm.fr

Abstract

OPA1 mutations are responsible for autosomal dominant optic atrophy (ADOA), a progressive blinding disease characterized by retinal ganglion cell (RGC) degeneration and large phenotypic variations, the underlying mechanisms of which are poorly understood. OPA1 encodes a mitochondrial protein with essential biological functions, its main roles residing in the control of mitochondrial membrane dynamics as a pro-fusion protein and prevention of apoptosis. Considering recent findings showing the importance of the mitochondrial fusion process and the involvement of OPA1 in controlling steroidogenesis, we tested the hypothesis of deregulated steroid production in retina due to a disease-causing *OPA1* mutation and its contribution to the visual phenotypic variations. Using the mouse model carrying the human recurrent *OPA1* mutation, we disclosed that Opa1 haploinsufficiency leads to very high circulating levels of steroid precursor pregnenolone in females, causing an early-onset vision loss, abolished by ovariectomy. In addition, steroid production in retina is also increased which, in conjunction with high circulating levels, impairs estrogen receptor expression and mitochondrial respiratory complex IV activity, promoting RGC apoptosis in females. We further demonstrate the involvement of Muller glial cells as increased pregnenolone production in female cells is noxious and compromises their role in supporting RGC survival. In parallel, we analyzed

[†]Last authors contributed equally to this work.
Received: February 8, 2016. **Revised:** March 26, 2016. **Accepted:** April 12, 2016

ophthalmological data of a multicentre *OPA1* patient cohort and found that women undergo more severe visual loss at adolescence and greater progressive thinning of the retinal nerve fibres than males. Thus, we disclosed a gender-dependent effect on ADOA severity, involving for the first time steroids and Müller glial cells, responsible for RGC degeneration.

Introduction

Autosomal dominant optic atrophy (ADOA) is a slowly progressive disease typically diagnosed during childhood. ADOA is characterized by a retinal ganglion cell (RGC) degeneration and loss of retinal nerve fibres, leading to reduced visual acuity (1). This blinding disease is in most cases due to mutations in *OPA1*, a gene encoding a mitochondrial GTPase essential for mitochondrial dynamics, maintenance of the mitochondrial DNA and regulation of apoptosis (2–4). The majority of *OPA1* patients present isolated optic neuropathy, but a subpopulation of them show extended clinical spectrum including deafness, myopathy, peripheral neuropathy known as ADOA$^+$ phenotype (5–7), as well as recently reported, parkinsonism and dementia (8). Additionally, there are also intra-familial and inter-familial variations in severity of the disease among patients with the same mutation. Despite important advances related to the OPA1 roles in mitochondrial physiology, little is known about how its mutations lead to neuronal loss, and no clear explanation for the large phenotypic variations has been proposed, rendering phenotype-genotype correlations arduous. Recently, we described the phenotype of the *Opa1* mouse model carrying the recurrent c.2708delTTAG mutation present in 20–30% of ADOA patients. We found that heterozygous mice displayed various degrees of neuronal and muscular alterations reflecting multisystemic degenerative symptoms, which reproduce syndromic ADOA$^+$ (9). Interestingly, re-assessment of phenotypic and molecular pathological parameters considering sexes revealed some clues for early and severe visual phenotype in females. Thus, we explored intrinsic mechanisms which could contribute to this phenotypic variability as clinical and biological factors influencing the visual outcome in ADOA are not well known, except for aging, which is associated with progressive visual loss (10). Recent studies have suggested the influence of sex steroids on brain mitochondrial metabolism and retinal function (11–13). Moreover, mitochondria are essential sites for steroid-hormone synthesis (14), and the importance of the mitochondrial fusion in this process has been demonstrated (15) with the involvement of OPA1 in the steroidogenic machinery (16,17). Although several large ADOA series have been studied for many clinical criteria, the influence of gender on ADOA visual outcome has not yet been raised (10,18–20). Consequently, we tested the hypothesis of a sex-dependent visual phenotype in ADOA. For this purpose, we explored the visual function as well as the retinal histology and metabolism of the *Opa1*^{delTTAG} mouse considering age, sex and ovariectomy. In parallel, we performed a reassessment of two relevant ophthalmological parameters, i.e. the visual acuity and the retinal nerve fibre layer (RNFL) thickness, on a large *OPA1* patient cohort with emphasis on gender. Here, we demonstrate the existence of a sex-dependent vision loss in female *Opa1* mice characterized by an early loss of visual acuity and RGC degeneration, which were abolished by ovariectomy. Further, we found that the *Opa1*^{delTTAG} mutation, by interfering with steroidogenesis process, impacts the visual phenotype in a sex-dependent manner. Finally, using a cross-sectional analysis of *OPA1* patient clinical data, we revealed an increased severity of the vision loss at adolescence and a greater progressive retinal nerve fibre decrease in women, not related to the most severe dominant negative mutations in *OPA1*, supporting the existence of a sex-dependent visual phenotype in ADOA.

Results

Opa1^{delTTAG} mutation leads to earlier onset of visual phenotype in female mice

To address our hypothesis of sex differences in ADOA, we performed a deep exploration of the visual phenotype in the *Opa1*^{delTTAG} mouse model taking into account age and sexes. Based on our previous data, and with the exception of electrophysiological measurements, we focused our observations on the age of phenotype appearance and on a late stage of the disease, i.e. 5 and 11 months. First, we assessed the visual function by analyzing visual-evoked potential (VEP) recordings. When compared with controls, *Opa1*$^{+/-}$ females displayed significant increased N- and P-wave latencies starting at 9 and 6 months, respectively, whereas *Opa1*$^{+/-}$ males only displayed an increased P-wave latency at the latest time-point of 13 months (Fig. 1A). VEP amplitudes were, however, not significantly affected in both *Opa1*$^{+/-}$ males and females versus controls (data not shown). At 5 months of age, mouse visual acuity assessment showed reduced capacity in *Opa1*$^{+/-}$ females, while it was unaffected in *Opa1*$^{+/-}$ males (Fig. 1B). At 11 months of age, both sexes had a visual acuity decrease of similar levels. Then, we performed retinal thickness measurements using Optical Coherence Tomography (OCT) and showed a progressive increase of the RNFL and of the inner plexiform layer in *Opa1*$^{+/-}$ females, becoming statistically significant at 11 months, while not in males (Fig. 1C and D). Peripapillary OCT measurements confirmed RNFL thickening in *Opa1*$^{+/-}$ females (Fig. 1E), which was associated with the presence of a noticeable edema evocative of an excitotoxic swelling of inner retinal layers (Fig. 1F). Finally, although both *Opa1*$^{+/-}$ males and females displayed significant similar RGC loss at 11 months, females displayed an earlier and exacerbated RGC degeneration readily observable at 5 months (Fig. 1G). Thus, exploration in mouse revealed earlier onset of retinal structure alterations and visual dysfunctions in *Opa1*$^{+/-}$ females compared with *Opa1*$^{+/-}$ males, reaching later a similar severity in both sexes. These results disclosed the early onset of visual phenotype in females, which emphasizes a putative role of sex steroids in modulating retinal functions and raises the question of the *Opa1*^{delTTAG} mutation effect on sex steroid production.

Opa1^{delTTAG} mutation leads to increased steroidogenesis in retina and blood

To investigate whether sex differences in ADOA visual phenotype may result from the lack of Opa1, we carried out hormonal assays in *Opa1* mice by focusing our experiments at 5 months, i.e. when the diseased phenotype has appeared in females while not yet in males.

We first monitored neurosteroidogenesis metabolic pathway in the retina by measuring the production of pregnenolone

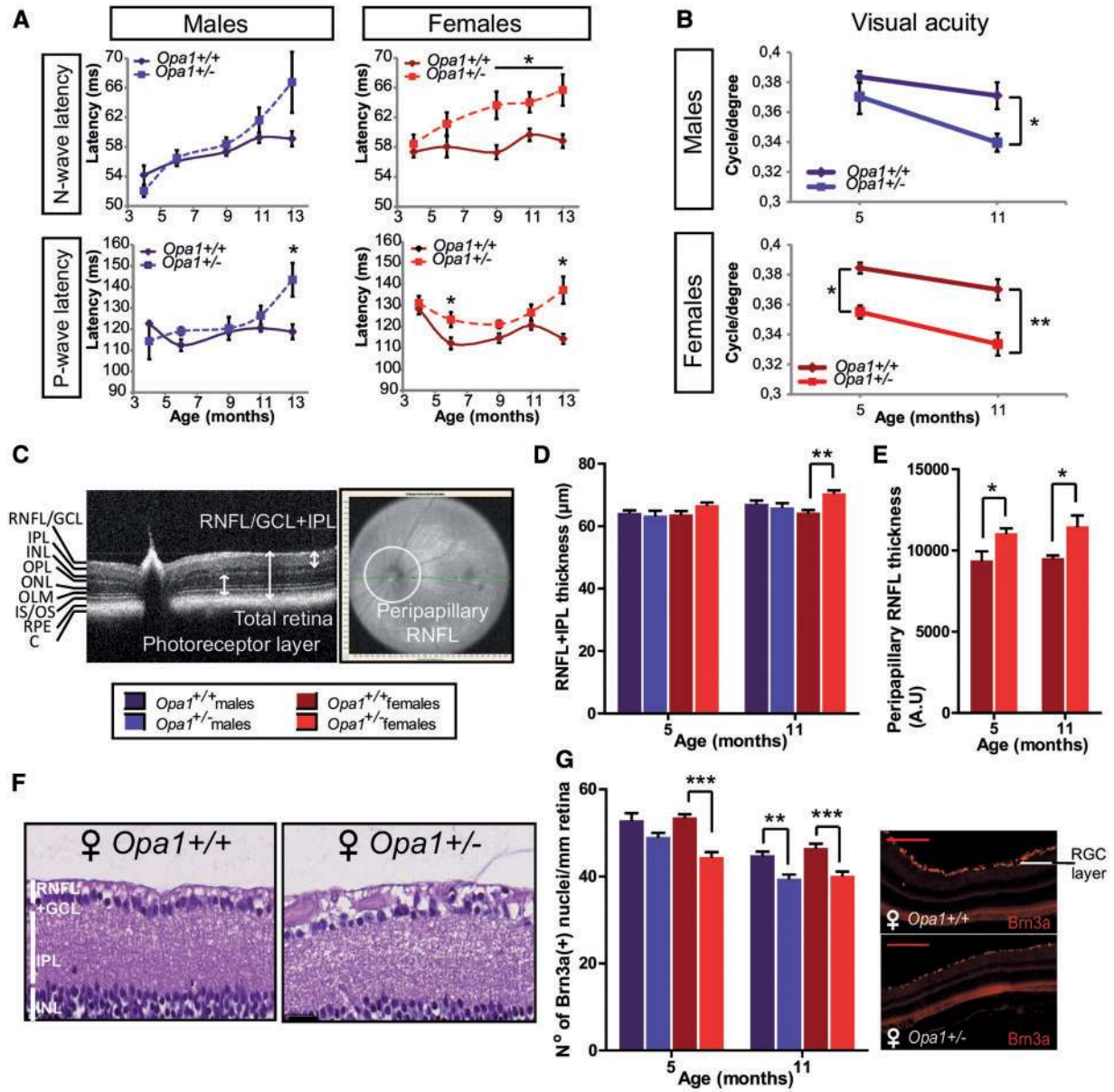

Figure 1. Functional and histological exploration of the Opa1^{delTTAG} mouse visual phenotype disclose early onset in Opa1$^{+/-}$ females. **(A)** Electrophysiological recordings of VEP N- and P-wave latencies in *Opa1*$^{+/+}$ and *Opa1*$^{+/-}$ male (Left) and female (Right) mice ($n = 3$–7/sex/genotype). **(B)** Visual acuity assessments on 5- and 11-month-old male (Top) and female (Bottom) *Opa1*$^{+/+}$ and *Opa1*$^{+/-}$ mice ($n = 5$–11/sex/genotype). **(C)** OCT assessments of retinal layers (Left) and retinal nerve fibre layer (RNFL, Right). RNFL/GCL, nerve fibre layer and ganglion cell layer; IPL, inner plexiform layer; INL, inner nuclear layer; OPL, outer plexiform layer; ONL, outer nuclear layer; OLM, outer limiting membrane; IS/OS: inner/outer segment; RPE, retinal pigment epithelium; C, choroid. **(D)** RNFL plus IPL thickness measurements on 5- and 11-month-old mice. **(E)** Female peripapillary RNFL thickness was determined as RNFL area calculation per field analyzed ($n = 5$–11/sex/genotype). **(F)** Representative picture of retinal cross sections stained with hematoxylin/eosin from 11-month-old *Opa1*$^{+/+}$ (Left) and *Opa1*$^{+/-}$ (Right) females ($n = 4$/genotype), scale bar = 25 µm. **(G)** RGC counting (Left) using a specific Red Brn3a immunolabelling (Right) was performed on retinal cross sections of 5- and 11-month-old mice ($n = 4$/sex/genotype). Data represent mean ± SEM. *$P < 0.05$, **$P < 0.01$ and ***$P < 0.001$ using one-way ANOVA (B,D,E,G) and Mann Whitney U test (A).

(PREG), the steroid precursor resulting from the first step of steroidogenesis in mitochondria. We monitored the basal and the maximal PREG production which reflected respectively the quality of cholesterol import and the CYP11A1 activity, the enzyme responsible for pregnenolone synthesis from cholesterol. We showed increased PREG basal production in *Opa1*$^{+/-}$ male and female retinas, although the maximal production remained unchanged (Fig. 2A). We also monitored the basal production of 17-beta estradiol, one of the main sex steroid produced in retina at the end of steroidogenesis. We found that both male and female *Opa1*$^{+/-}$ retinas displayed increased 17-beta estradiol production (Fig 2B), which was nevertheless much higher in *Opa1*$^{+/-}$ females than in males. These results demonstrated that the *Opa1*^{delTTAG} mutation alters the efficiency of steroidogenesis and results in abnormally increased levels of PREG and 17-beta estradiol in both male and female heterozygous retinas.

The difference in this retinal hormonal deregulation between male and female *Opa1*$^{+/-}$ mice probably does not explain by the sex-dependent retinal alterations and disease onset. Thus to go further, we performed PREG assays in blood serum samples from *Opa1* mice. Results showed a 21-fold increase in *Opa1*$^{+/-}$ female serum compared with controls

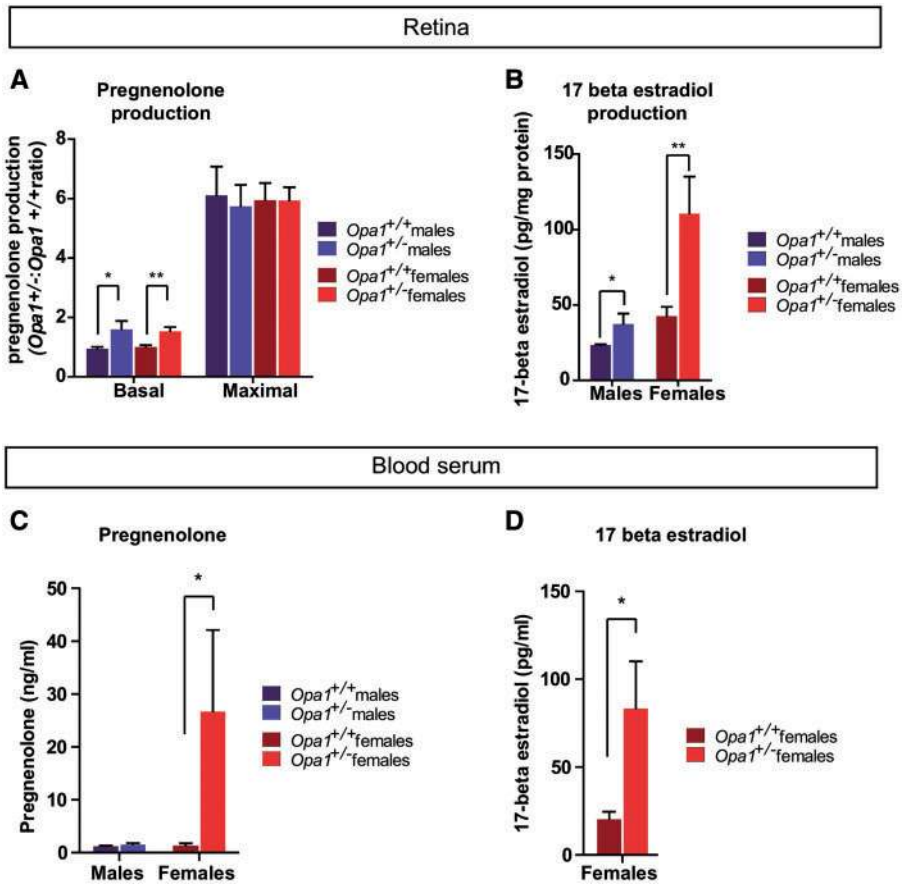

Figure 2. *Opa1*^{delTTAG} mutation impacts the steroidogenesis efficiency and leads to increased retinal and circulating sex steroid production. All experiments were performed on 5-month-old *Opa1* mice. **(A)** Basal and maximal pregnenolone productions were quantified in retinal explant supernatants from both male and female mice. Data are expressed related to retinal protein content and to control mouse basal values ($n = 4$–14/sex/genotype). **(B)** 17-beta estradiol basal production was quantified in retinal explant supernatants from both male and female mice. Data are expressed related to the retinal protein content ($n = 4$–14/sex/genotype). **(C)** Blood serum pregnenolone assays in both male and female mice ($n = 4$–7/sex/genotype). **(D)** Blood serum 17-beta estradiol assays from female mice ($n = 5$/sex/genotype). Data represent mean ± SEM. *$P < 0.05$ and **$P < 0.01$ using one-way ANOVA **(B,C,D)** and Mann Whitney U-test (A).

(26.68 ± 15.4 ng/ml versus 1.27 ± 0.47), whereas similar low PREG levels (1.52 ± 0.26 ng/ml versus 1.19 ± 0.13) were observed in *Opa1*$^{+/-}$ and control males (Fig. 2C). We also quantified 17-beta estradiol in *Opa1*$^{+/-}$ female serum and found a significant increase of circulating levels compared with wild-type serum (Fig. 2D). Thus, we disclosed the existence of deregulated circulating levels of pregnenolone and 17-beta estradiol in *Opa1*$^{+/-}$ females, suggesting that Opa1 haploinsufficiency affects the production of the circulating sex steroids, mainly produced by ovaries.

Ovariectomy abolishes sex differences and early onset of visual phenotype

To estimate the influence of ovarian circulating sex steroids on the visual phenotype expressivity, we ovariectomized wild-type and *Opa1*$^{+/-}$ mice at 3 weeks of age. Following this surgery, the *Opa1*$^{+/-}$ related weight loss evidenced from the age of 6 months was abolished (Fig. 3A). Then, while ovariectomy (*Ovx*) did not affect the N-wave latency, we showed that *Ovx Opa1*$^{+/-}$ displayed increased P-wave latency only at 11 months (Fig. 3B). OCT measurements did not show any modification of the RNFL + IPL thickness (Fig. 3C), but significant RGC loss was found in *Ovx Opa1*$^{+/-}$ also only at 11 months (Fig. 3D). Taken together, these results demonstrated that ovariectomy abolishes sex differences observed in visual phenotype between males and females, and delays the disease onset at a time similar to that of males. This finding confirmed the influence of sex steroids in the modulation of retinal functions and moreover, pointed to a negative impact of excessive circulating female sex steroids on retinal metabolism.

Opa1^{delTTAG} -induced steroid deregulation leads to early mitochondrial complex IV defect in female retinas

Previously, we disclosed that the *Opa1*^{delTTAG} mutation altered the mitochondrial respiratory chain leading to a cytochrome c oxidase (complex IV) enzymatic activity deficiency. In the line of these results, we studied whether abnormal increased circulating and retinal steroids levels could alter the complex IV activity in the retina. Thus, we monitored mitochondrial complex IV and citrate synthase activities considering sexes. Interestingly, although no difference was found between male and female controls, a significant reduction in complex IV activity was found in *Opa1*$^{+/-}$ female retinas at 5 months (Table 1), while that of *Opa1*$^{+/-}$ male was only found affected later at 11 months (data not shown). In order to determine whether these

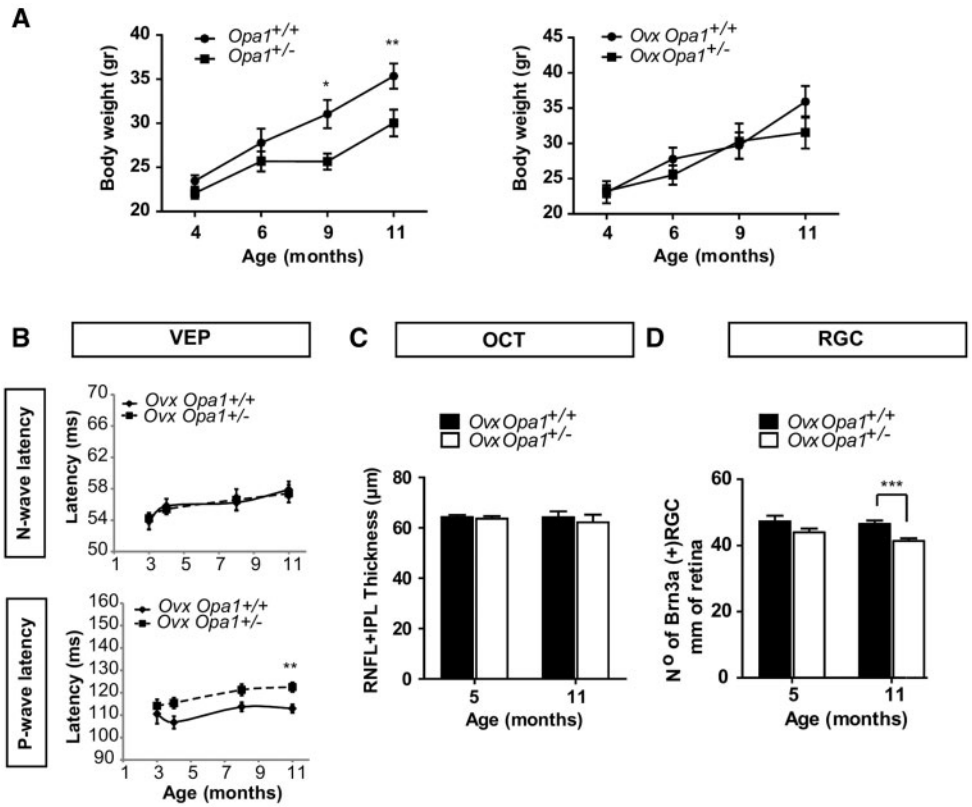

Figure 3. Ovariectomy abolishes sex differences in ADOA phenotype. Ovx, ovariectomized. **(A)** Body weight monitoring without (left) and following (right) ovariectomy. **(B)** VEP recordings show unaffected N-wave latency but increased P-wave latency at 11 months in *Ovx Opa1*$^{+/-}$ compared with *Ovx* controls ($n = 9$–11/sex/genotype). **(C)** OCT measurements do not show modification of RNFL + IPL thickness between control and *Ovx* animals ($n = 4$–7/sex and genotype). **(D)** Brn3a immunolabelling on cross retinal sections shows RGC loss at 11 months ($n = 5$–11/sex/genotype). Data represent mean ± SEM. $^{**}P < 0.05$ with Mann-Whitney U test (B), $^{**}P < 0.01$ and $^{***}P < 0.001$ using one-way ANOVA (A and D).

Table 1. Mitochondrial cytochrome c oxidase (CIV) and citrate synthase activities in 5-month-old Opa1$^{+/-}$ female retinas before and after ovariectomy

Sex	Genotype	Enzyme activity (nmol/min/mg protein)			P-value
		CIV	CS	CIV/CS	
Males	*Opa1*$^{+/+}$	780 ± 172.4	623 ± 104.1	1.246 ± 0.150	0.1143
	Opa1$^{+/-}$	500 ± 81.61	678 ± 83.41	0.751 ± 0.092	
Females	*Opa1*$^{+/+}$	446 ± 115.9	432 ± 71.2	**0.874 ± 0.053**	**0.0092****
	Opa1$^{+/-}$	155 ± 18.8	360 ± 26.7	**0.443 ± 0.053**	
***Ovx* Females**	*Opa1*$^{+/+}$	726 ± 131.5	3537 ± 705	0.210 ± 0.023	0.2879
	Opa1$^{+/-}$	897 ± 83.2	3543 ± 244	0.253 ± 0.0164	

CIV, mitochondrial complex IV or cytochrome c oxidase; CS, citrate synthase. Results statistically significant are specified in bold font ($n = 4$–7/sex/genotype). Data are expressed as mean ± SEM.

$^{**}P < 0.01$ using Mann Whitney U-test.

mitochondrial enzymatic activities undergo the influence of sex steroids, we repeated these experiments on mouse retinas after ovariectomy. Remarkably, we found that ovariectomy increased drastically citrate synthase activity in both control and *Opa1*$^{+/-}$ retinas. As previously observed for functional and histological parameters following ovariectomy, mitochondrial complex IV activity reached normal values in *Opa1*$^{+/-}$ female retinas (Table 1). Thus, these results demonstrated the early onset of mitochondrial complex IV defect in female *Opa1*$^{+/-}$ retinas and showed that ovariectomy delays *Opa1*$^{+/-}$ female visual phenotype appearance to a time course similar to that of males, supporting the negative impact of circulating female sex steroids on the retinal mitochondrial metabolism.

Retinal and circulating steroid deregulations impact on retinal steroidogenic metabolism and RGC survival

We further studied the consequences of cumulative circulating and retinal pregnenolone and 17-beta estradiol increases on the mitochondrial steroidogenic metabolism in retina. First, we quantified the mRNA expression of the *StAR* gene, which encodes a crucial protein regulating cholesterol transfer into

mitochondria. We found that StAR expression did not change between sexes and genotypes (Fig. 4A). We also studied the expression of genes encoding mitochondrial steroidogenic enzymes as *Cyp11a1* and *3βHSD1*, encoding the 3β-hydroxysteroid dehydrogenase type 1. In contrast with *StAR* expression, we found an up-regulation of *Cyp1a11* and *3βHSD1* expressions in *Opa1*$^{+/-}$ female retinas compared with female controls (Fig. 4A). Then, we monitored the expression of Estrogen Receptors (ERs) in the retina (Fig. 4B) and found that *Esr2* expression is 50-fold higher than that of *Esr1* in control retinas. Remarkably, while no differences were found between control and *Opa1*$^{+/-}$ male mice, we observed an up-regulation of *Esr1* and a down-regulation of *Esr2* mRNA expressions in *Opa1*$^{+/-}$ female retinas compared with controls (Fig. 4B). Finally, in this context of deregulated steroid levels and earlier female disease onset, we found higher levels of TUNEL positive RGCs in female retinas compared with controls (Fig. 4C). Specific RGC TUNEL identification was confirmed with the Brn3a co-immunolabelling (data not shown). Our results showed that increased retinal and circulating levels in pregnenolone and 17-beta estradiol affect mitochondrial steroidogenesis efficiency and alter ER-dependent regulations specifically in *Opa1*$^{+/-}$ females, promoting earlier RGC apoptosis.

Early deleterious steroidogenesis deregulation occurs in female Müller glial cells

In order to evaluate whether RGC cellular environment is affected by excessive retinal and circulating steroid levels, we studied Müller glial cells. Indeed, these cells are crucial for RGCs as they are in contact with retinal blood vessels, receiving circulating steroids and participate to retinal neurosteroid production. In addition to this steroidogenic support, Müller glial cells exert a crucial role in removing extracellular glutamate, which is critical for RGC functioning and survival. The study of primary cultures of postnatal day 10 Müller cells from both *Opa1*$^{+/-}$ males and females evidenced a fissioned mitochondrial network (Fig. 5A). Before performing hormonal assays, we validated the intrinsic capacity of Müller cells to produce PREG with the

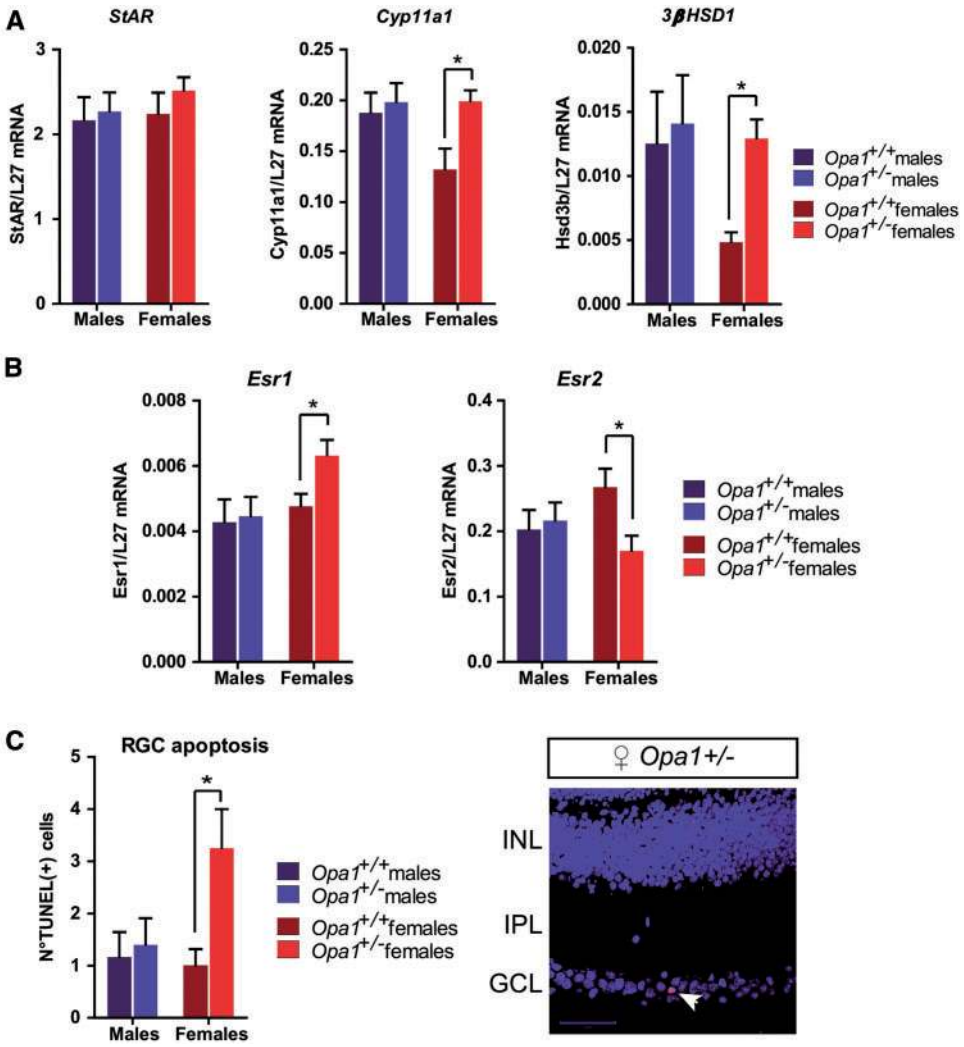

Figure 4. Cumulative retinal and circulating steroid overproductions alter retinal mitochondrial steroidogenic metabolism and RGC survival. All experiments were performed on 5-month-old *Opa1* retinas. **(A)** Quantification of steroidogenic gene expressions by real-time quantitative PCR ($n = 4$–6/sex/genotype). **(B)** Quantification of ER expressions by real-time quantitative PCR experiments ($n = 4$–6/sex/genotype). **(C)** Apoptotic RGC counting (left) was done in retinal cross sections (right). Data were expressed in percentage of red TUNEL positive RGCs observed by confocal microscopy (arrow head on the right panel), INL, inner nuclear layer; IPL, inner plexiform layer; GCL, ganglion cell layer ($n = 4$–7/sex/genotype). Data represent mean ± SEM. *$P < 0.05$ and **$P < 0.01$ using one-way ANOVA (C) and Mann Whitney U-test (A,B).

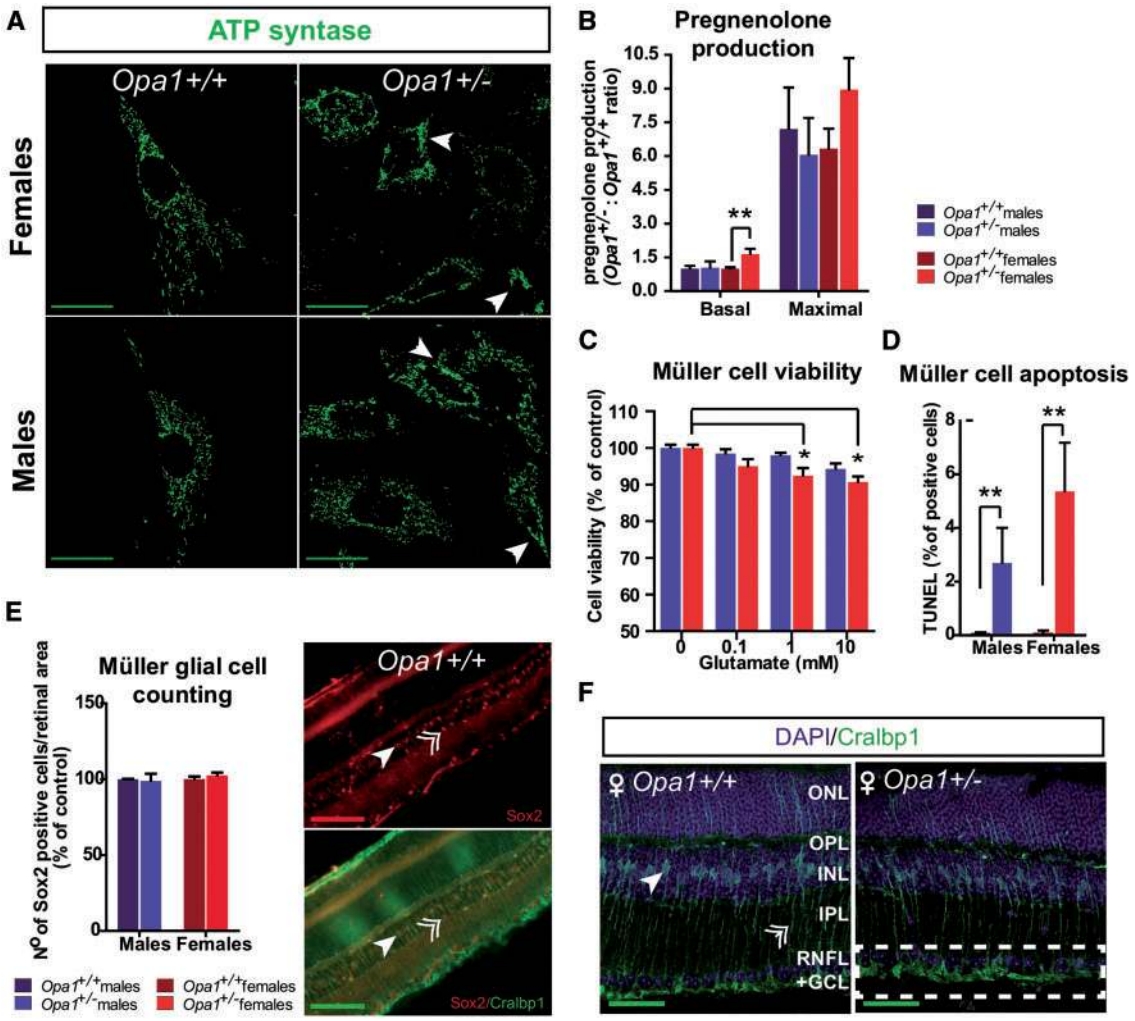

Figure 5. Early deleterious effect of pregnenolone overproduction in female Opa1$^{+/-}$ Müller glial cells. **(A)** Assessment of the mitochondrial network structure using ATP synthase immunolabelling (in green) on Müller glial cell primary cultures, obtained from retinas of postnatal day 10 mice. Arrow heads point to abnormal mitochondrial aggregates. **(B)** Pregnenolone basal and maximal productions were measured in supernatants of Müller glial cell primary cultures ($n = 6$–10/sex/genotype), data are expressed as the ratio of *Opa1*$^{+/-}$ values related to *Opa1*$^{+/+}$ basal values. **(C)** Assessment of cell viability from a glutamate dose response (0, 0.1, 1 and 10 mM) experiment performed on Müller cell primary cultures. Data are expressed as the percentage of control Müller cell viability from three independent experiments. **(D)** Assessment of Müller glial cell apoptosis in primary cultures expressed in percentage of red TUNEL positive cells observed by confocal microscopy. **(E)** Müller glial cell counting (left) using a nuclear Sox2 antibody immunostaining on 5-month-old cross retinal sections (right). Specificity of Sox2 labelling was confirmed with Cralbp1 co-immunolabelling (Right). Arrow head: Müller cell nucleus, double arrow head: cholinergic amacrine nucleus ($n = 4$/sex/genotype). **(F)** Cralbp1 immunolabelling on retinal cross sections of 5-month-old mice reveals Müller cells (arrow head: soma; double arrow head: cytoplasmic arm) and their endfeet (between doted frame). Data represent mean ± SEM. *$P < 0.05$ and **$P < 0.001$, using one-way ANOVA.

quantification of the *Cyp11a1* gene expression in Müller cell cultures (data not shown). We then measured PREG production and disclosed an increased basal PREG production in *Opa1*$^{+/-}$ female cells compared with that of wild-type and male cells, while maximal production was also found unchanged (Fig. 5B). Then, unlike *Opa1*$^{+/-}$ male cells, we found that the viability of *Opa1*$^{+/-}$ female cells was impacted by increased glutamate concentrations (Fig. 5C). Although we found significant level of TUNEL positive apoptotic cells in both male and female *Opa1*$^{+/-}$ cells compared with controls, a higher level of apoptosis was observed in female cells (Fig. 5D). Exploration of 5-month-old *in vivo* retinas disclosed that the specific Sox2 labelling did not reveal any quantitative modification of the Müller glial cell number (Fig. 5E). In contrast, assessment of Müller glial cell morphology, using Cralbp1 Müller immuno-labelling, revealed endfoot swelling specifically in female retinas (Fig. 5F). Thus, these results showed that *Opa1*^{delTTAG} mutation alters steroidogenesis in female Müller glial cells and leads to toxic pregnenolone overproduction, inducing stress-related modifications of their cellular appearance and sensitizing them to apoptosis.

OPA1 female patients display an earlier and a more severe visual phenotype than male patients

To address the question of a gender difference in ADOA patients, we analyzed ophthalmological data from 154 non-syndromic ADOA patients with an *OPA1* mutation recruited in three reference centres. Clinical data were stratified into three age groups: <20-years old (yo), between 20 and 45 yo and over 45 yo (Table 2). First, we analyzed the best-corrected visual acuity data, considered here as the logarithm of the minimum angle of resolution (LogMAR). In accordance with the progressive

evolution of the disease, we observed a progressive decrease in visual acuity with age in male patients as shown by logMAR values increasing with time (Fig. 6A). By contrast, female vision loss did not reveal any significant evolution. Nevertheless, female patients younger than 20 yo displayed a significantly higher diminution of visual acuity compared with young males, reaching values observed only for males >45 yo (Fig. 6A). When the group of youngest patients was split into two groups (<11 and 11–19 yo), we found that only pubescent females were statistically different from males of the same age (data not shown). Then, we reassessed clinical data obtained from the RNFL thickness measurements around the optic disc, which reflects the RGC number. We found that the RNFL was already reduced in young *OPA1* patients and slimmed down progressively with age in both males and females (Fig. 6B, normal value = 110 μm ± 5 in healthy subjects). In the group of eldest patients, a higher RNFL loss was found in females compared with males, and this difference was even more significant when considering all groups together (Fig. 6C). Although results from the visual acuity reassessment suggested an earlier increase of disease severity in females, we found a more severe clinical presentation with greater progressive retinal nerve fibre degeneration in female than in male patients, when considering altogether the 154 *OPA1* patients. Finally considering that dominant negative mutations of OPA1 GTPase domain result in more severe clinical presentations, we tested whether the gender-dependent severity observed could be influenced by the mutational status (Table 3). In younger patients, dominant negative mutations in the GTPase domain account for 36% in female versus 39% in male patients. Conversely, mutations leading to premature frameshifts and thus to haploinsufficiency are predominant in these groups and the others, representing the main mutation type in our cohort (69.3% in females versus 74.4 in males).

Table 2. Cross-sectional analysis of 154 OPA1 patients

OPA1 patients		
Age (years)	**Females (*n*)**	**Males (*n*)**
Total	78	83
Average	35 ± 11.2	33.6 ± 10.1
<20	11	23
Average	12.9 ± 1.5	13.1 ± 0.8
20–45	33	34
Average	32.1 ± 1.3	31.6 ± 1.3
>45	31	21
Average	60.0 ± 1.7	56.0 ± 1.3

Patients are classified in three different groups: before the age of 20 yo, between 20 and 45 yo and over 45 yo. In each group, males and females are studied separately.

Discussion

Since the initial description of patients with dominant optic atrophy, it has been a main concern to explain the wide panel of severity among affected persons. This rendered phenotype—genotype studies tedious, as a same *OPA1* mutation, for example the common c.2708delTTAG mutation, could lead to asymptomatic patients or to severely affected syndromic cases. Genetic analyses intending to identify secondary markers, and in

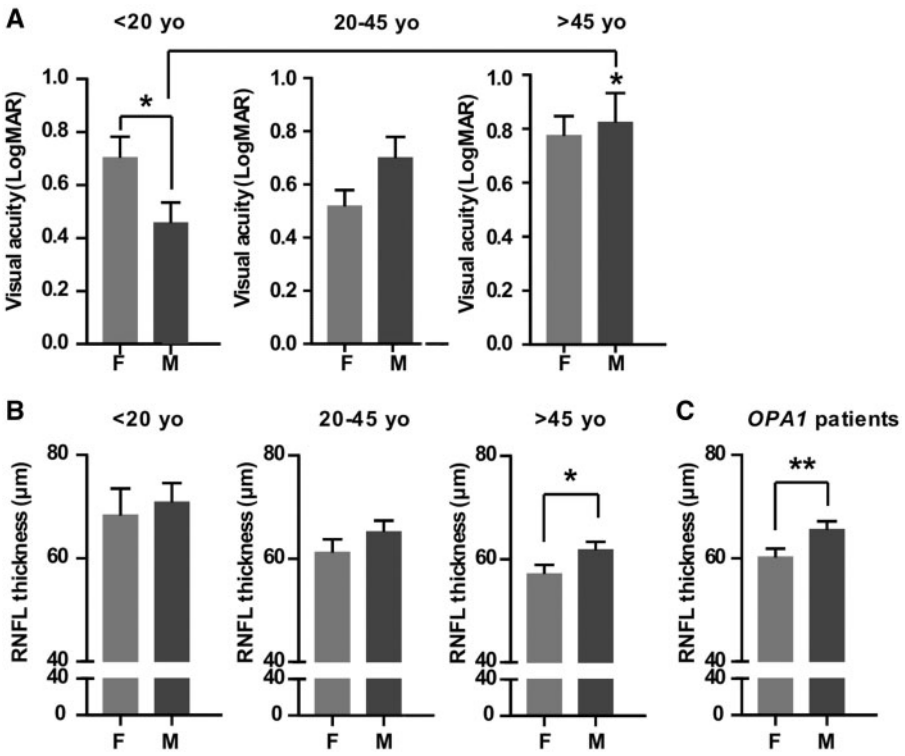

Figure 6. Cross sectional analysis reveals early and more severe ophthalmological phenotype in female ADOA patients. 154 OPA1 patients were separated in three groups according to their age: young patients <20 yo, adults (20–45 yo) and seniors (>45 yo) (see also Table 2) F: female, M: males. **(A)** Mean visual acuity expressed as the logarithm of the minimum angle of resolution in minutes of arc (LogMAR, 0.0 = 1.0 decimal (normal visual acuity), 1 = 0.1 decimal (level of social blindness). **(B)** Mean RNFL thickness assessed by OCT in the <20 yo, 20–45 yo and >45 yo groups **(C)** Mean RNFL thickness considering all females and all males together. Data represent mean ± SEM. *$P < 0.05$ and **$P < 0.01$ using one-way ANOVA.

Table 3. Percentage of dominant negative and haploinsufficient mutations in the OPA1 patient cohort

Mutation	Females				Males			
Percentage (%)	**Total**	<20	20–45	>45	**Total**	<20	20–45	>45
Dominant negative (GTPase domain)	**21.3**	36.4	15.2	22.6	**19.2**	39	14.7	4.8
Haploinsufficiency (frameshift)	**69.3**	54.5	72.7	71	**74.4**	52.2	79.4	90.5

Dominant mutations in the GTPase domain are reported. Haploinsufficient mutations gather mutations leading to premature frameshift. Results are expressed in percentage.

particular the contribution of the mitochondrial DNA haplogroup, have not allowed solving this conundrum suggesting that environmental or systemic parameters could modulate ADOA severity (21).

The study presented here has been inspired from previous observations gathered on the *Opa1*^{delTTAG} mouse that suggested the presence of sex differences in the visual phenotype of heterozygous mice. Consequently, the deep exploration of this mouse revealed an earlier onset of vision loss in female than male *Opa1* mice. Furthermore, we disclosed that Opa1 haploinsufficiency, by early altering steroidogenesis efficiency, leads to abnormal high steroid levels, which impair mitochondrial metabolism in retina and predispose females to early vision loss. Indeed, we confirmed the involvement of Opa1 in the control of steroidogenesis efficiency as its haploinsufficiency results, in both *Opa1*$^{+/-}$ male and female retinas, in increased pregnenolone production, the mitochondrial steroid precursor, as well as 17-beta estradiol, the major end product of this pathway. Moreover, the fact that Opa1 interferes with the basal pregnenolone production without modification of the maximal production, reflecting the CYP11A1 enzyme activity, supports recent findings showing that *in vitro* OPA1 silencing enhances steroidogenesis efficiency by regulating cholesterol import through mitochondrial membranes. Indeed, OPA1 has been found to belong to the transduceosome, a multi-protein complex required for mitochondrial cholesterol trafficking and cleavage into pregnenolone by the CYP11A1 enzyme (16,17). Thus, in pathological conditions, pregnenolone and neurosteroid synthesis might consequently be stimulated in gonads to produce steroid hormones, and in the central nervous system, among which the retina. This might lead to key consequences on the brain structures and functions, as pregnenolone is the most abundant steroid in this organ and is crucial for the modulation and the protection of neuronal activities (13,22–24), and contributes to sex-dependent mitochondrial functions (11). It has also key consequences on the retinal functions, as pregnenolone synthesis is abundant in the inner nuclear and ganglion cell layers, where interneurons, Müller glial cells and RGCs not only synthetize this steroid, but also depend upon its level to modulate their activity (22,25,26).

These data raise a first question concerning the effects of steroid overproduction on the retinal function and structure. Indeed, the difference observed in steroid deregulation between *Opa1*$^{+/-}$ male and female retinas cannot explain by itself the sex-dependent retinal alterations and the early disease onset in females. Actually, we disclosed specifically in females a drastic increase in pregnenolone and 17-beta estradiol circulating levels, which suggests that Opa1 insufficiency impairs the ovarian steroidogenesis. In addition, the fact that ovariectomy abolishes sex differences observed in visual phenotype confirms that sex steroids produced by ovaries modulate the retinal function and points undeniably to a negative impact of excessive circulating female sex steroids on vision.

A second question concerns the mechanism by which high circulating steroid levels affects RGC structure and functions. Our data suggest that circulating steroids impact negatively the RGC mitochondrial metabolism, in particular the activity of the respiratory complex IV, compromising RGC physiology. Although 17-beta estradiol is known to induce a neuroprotective effect in physiological conditions, its 4-fold increase together with a 21-fold increase in pregnenolone in *Opa1*$^{+/-}$ female blood must lead to a noxious effect on the inner retinal neurons, maybe through deregulation of ER activation that are mostly expressed in retinal inner layers especially in RGC (12,25). In this respect, considering the capacity of pregnenolone to activate ERs (27), modification of *Esr1* and *Esr2* gene expressions found in retina could represent an adaptive response, as already reported in response to long-term estrogen treatment notably in brain visual regions (28–31). Interestingly, Esr2 is almost exclusively localized in mitochondria (32) to regulate mitochondrial function, partly through the regulation of mitochondrial complex IV subunit mRNA expression (33). It is further known that *Esr2* down-regulation correlates with reduced mitochondrial respiratory complex IV activity, what we observed specifically in retina from *Opa1*$^{+/-}$ females (34). Thus, these results suggest that quantitative and regulatory modifications of the retinal ERs in response to excessive steroid levels impact the retinal mitochondrial metabolism from *Opa1*$^{+/-}$ females compromising RGC functions and survival.

The third question concerns the effects of the retinal production of steroids on the direct environment of RGCs. Indeed, the study of Müller glial cells that are essential for RGC functioning and survival (25,35), revealed increased pregnenolone basal production, together with a higher response to glutamate excitotoxicity and a greater level of apoptotic death, specifically in cells purified from *Opa1*$^{+/-}$ females. Accumulation in retina of pregnenolone triggers excitotoxicity by induction of NMDA receptors, leading to ganglion cell layer swelling and RGC apoptosis, while NMDA receptor activation stimulates in turn pregnenolone synthesis, potentiating its excitotoxic effects (36–38). *Cyp11a1* and *3βHSD1* up-regulations specifically found in *Opa1*$^{+/-}$ females support the existence of this vicious cycle and probably contribute to explain the higher increase in 17-beta estradiol in female retinas. These data suggest the toxicity of pregnenolone overproduction which, by increasing Müller cell sensitivity to glutamate, promotes endfoot swelling formation around RGC soma *in vivo*. This latter observation could explain the increased RNFL thickness found by OCT measurements, and contribute to RGC dysfunction and susceptibility to premature cell death, especially in *Opa1*$^{+/-}$ females. Remarkably, these results reveal the involvement of Müller glial cells in OPA1-related pathophysiology, a process probably occurring early in the development of the disease, i.e. in the post-natal period.

Altogether, results found in mouse confirm the existence of a sex-dependent visual phenotype, reported for the first time in ADOA. The underlying mechanism responsible for this process

is related primarily to *Opa1* haploinsufficiency which, by significantly enhancing steroidogenesis, leads to the accumulation of deleterious high circulating and retinal steroid levels. Our results collected from a retrospective analysis of ophthalmological data from 154 *OPA1* patients supported the hypothesis of a sex-dependent visual phenotype, with an earlier and more severe vision loss in females than in males. Indeed, although male patients displayed a progressive visual acuity decrease with age, females presented an increased severity of visual acuity before the age of 20, which straightaway reached a severity similar to the one found in oldest male group. In parallel, *OPA1* female patients harbored a greater loss in retinal nerve fibres, reflecting RGC degeneration. Thus these results suggest that adolescence is a critical period influencing the loss of visual acuity in young ADOA females, evoking a negative influence of sex steroids, produced massively during puberty and later with lifelong cyclic fluctuations. In this line, the increased severity observed in female patients is further supported by the fact that *CYP11A1* expression and circulating pregnenolone reach high levels during female puberty, and vary according to lifelong female hormonal cycle (39,40). Moreover, the fact that young females develop an earlier and a more severe decrease in visual acuity, while both young males and females harbored the same level of RGC degeneration, supports the concept that sex steroids modulate retinal and RGC functions favouring, with time, greater RGC degeneration in females. Finally, the inventory of dominant negative versus haploinsufficient mutations provided an additional insight in the consideration of DOA severity. Indeed, the lower amount of dominant negative mutations in the young female group reduced their eventual impact in controlling the severity of the disease found in this specific group. Both in mouse and human, our results emphasize a causative effect of OPA1 haploinsufficiency.

Thus, our data warrant prospective clinical studies in which the number of young subjects should be increased and various parameters such as pubertal development, pregnancies, exposure to contraceptives and hormonal supplements, and circulating concentrations of steroid hormones should be carefully considered in ADOA patients, in addition to their ophthalmological examination. In a more general consideration, our data also put emphasis on the role of mitochondrial physiology in the control of the neurosteroidogenesis pathway. A particular attention should be given to puberty since this is a critical period in lifetime, in which the novel hormonal status renders cells and tissues more dependent on mitochondrial energy metabolism. Therefore, impairment of neurosteroidogenesis should be considered as a pathophysiological mechanism that could be involved in other mitochondrial disorders affecting the central and peripheral nervous systems, in a sex dependent manner.

Finally, we extended the knowledge on the *OPA1*-related pathophysiology by providing the evidence of steroid deregulations impacting the visual phenotype in a sex-dependent manner. Moreover, we reveal the involvement of the Müller glia, in controlling the fate of RGC in ADOA. Thus, we provide new insights to explain some variability of the ADOA phenotype, which might lead to improved diagnosis approaches and therapeutic strategies in the near future.

Materials and Methods

Opa1^{delTTAG} mouse model

The *Opa1* knock-in mice carrying the c.2708_2711delTTAG mutation was described in Sarzi *et al* (9). Mice were kept in the animal facility of the Institute for Neurosciences of Montpellier (B 3417236, March 11, 2010). All protocols were carried out on males and females *Opa1*$^{+/-}$ mice and their *Opa1*$^{+/+}$ littermates.

Examination of the visual electrophysiology

Every 2–3 months, VEPs were performed on anesthetized mice and recorded using three phases of 60 flashes as previously described in (41). Flash duration was 5 ms with a frequency of 1 Hz and intensity of 159 cd.s^{-1}.m^{-2}. Amplitudes and latencies obtained during each phase were averaged. A cut-off filter was set at 35 Hz.

Virtual-reality optokinetic system

Mouse visual acuity was assessed as described by Prusky *et al.*, 2004 (42). The apparatus included a virtual optomotor constituted by four computer monitors arranged in a quadrangle arena generating a virtual rotating cylinder with drifting vertical sine wave grating. The OptoMotry (Cerebral Mechanics, Lethbride, Alberta, Canada) was used to control grating parameters and video recordings. Then, mice were placed on a central platform allowing them to track the grating with reflexive head and neck movements. The increasing of the grating frequency (from 0.042 to 0.442 cyc/deg) until the optomotor reflex could not be detectable, defined the visual acuity. Contrast sensitivity was given at the 0.042 cyc/deg frequency. Mice were tested for both eyes in the morning at the beginning of their daylight cycle. Experiments were done blind to the genotype.

Retinal cell counting

Mice were euthanized by cervical dislocation. Eyes still connected to their optic nerve were immediately frozen in isopentane cooled by liquid nitrogen and embedded in Tissue-Tek O.C.T. compound. For RGC counting, 14 μm cryostat sections were immunolabelled using a Brn3a primary antibody (1:500, Santa Cruz Biotechnology) along with an Alexa 594 conjugated anti-goat secondary antibody (1:800, Invitrogen, Oregon, USA). A Sox2 primary antibody (1:200, Santa Cruz Biotechnology) combined with an Alexa 594 conjugated anti-goat antibody was used to quantify Müller glial cell nuclei. Sections were scanned using the NanoZoomer 2.0-HT automatized microscope (Hamamatsu) or visualized by confocal microscopy (Zeiss LSM510 META). RGC counting was calculated as the ratio of the RGC number encountered related to the total retinal area per section. Müller cell counting was determined as the ratio of the Sox2 positive cell number to the interneuron layer area per section. Four sections per retina were analyzed.

Endocrine assays

Menstrual cycle synchronization was ensured using conjoined mice breeding from birth to sacrifice. Pregnenolone and 17-beta-estradiol assays were adapted from Wasilevski *et al.* (17) and carried out on *Opa1* mouse retinal explant supernatants as well as on Müller cell primary culture supernatants.

Pregnenolone assay

Müller glial cells (2×10^4) were seeded onto 24-well plate for 48 h in appropriate culture medium. Basal rate of pregnenolone production was assessed after 24 h incubation of cells in FBS-free DMEM-F12 culture medium containing trilostane (2 μg/ml,

Sigma). Maximal rate was then determined during 1-h incubation with trilostane and saturating concentration of 22(R)-hydroxycholesterol (0.5 μg/ml, Sigma). After removing the supernatant, cells were harvested and protein concentration determined by BCA colorimetric assay (Thermo Scientific Pierce). Pregnenolone was quantified by ELISA (IBL International GmbH). Retinal explants were incubated 2 h at 37 °C in Hanks Balanced Salt Solution (HBSS) in the presence of trilostane to measure basal pregnenolone production, then 1 h in HBSS containing both trilostane and 22(R)-hydroxycholesterol to assess maximal pregnenolone production.

17-beta-estradiol (E2) assay

E2 production was measured in retinal explant supernatants. Retinas were incubated 3 h at 37 °C in HBSS with 22(R)-hydroxycholesterol (0.5 μg/ml, Sigma). E2 was quantified by ELISA technique (Enzo Life Science). Circulating E2 was directly quantified on blood serum.

Mouse ovariectomy

Twenty-one-day old mice (12 wild-type and 11 heterozygous) were anesthetized by intra-peritoneal injections mixture of ketamine (120 mg/kg) and xylasine (10 mg/kg). Animals were placed on the dorsal position, shaved and cleaned. A ventral single midline skin incision was made halfway between the basis of the ribcage and the genital organ. A single incision was done into the muscle wall and each ovary was removed. Muscle and skin incisions were successively sutured with specific needle and surgical thread.

Mitochondrial enzymatic activities

Mitochondrial cytochrome c oxidase and citrate synthase activities were measured on retinal homogenates, at 37 °C using a Beckman DU-640B spectrophotometer (Beckman Coulter, CA, USA), and standard method (43).

Molecular characterization

Quantitative real-time PCRs were performed on total RNA extracted from retinas using the RiboPure Kit (Ambion, Inc.). One μg of RNA product was reverse-transcribed with the Verso cDNA Kit (Thermo Fisher Scientific Inc.) according to the manufacturer's instructions. *StAR, Cyp11a1*, *3βHSD1*, *Esr1* and *Esr2* transcripts were quantified using specific pairs of primers with SYBR Green/LightCycler technology (Roche) and reported to the ribosomal protein *L27* gene expression.

Müller glial cell primary cultures

Mouse primary retinal Muller cells were generated from 10-day-old neonatal *Opa1*^{delTTAG} pups. Animals were euthanized and their eyes enucleated. The globes were dissected and rinsed with HBSS. The anterior segment and vitreous were excised and the RPE layer removed. Retinas were transferred into DMEM-F12 containing 10% FBS and triturated several times with a pipette. Dissociated cells were transferred into 25 cm^2 flasks and grown at 37 °C for 4 days. After the mixed culture had grown confluent, flasks were rinsed twice with DPBS to remove loosely attached cells. Cells were trypsinized and split in new 25 cm^2 flasks to be further investigate at low passages (P3 to P6). Immunohistochemistry was done to estimate the Müller cell enrichment of primary cultures using a Cralbp1antibody (AGRO-BIO, France, 1:500) and using Gfap antibody (Dako, 1:1000) for astrocyte detection. The purity of Muller cells in our primary cultures exceeded 99%. Mitochondrial network was assessed using the ATP synthase antibody coupled with a secondary Alexa 488 anti-rabbit antibody (1:500, Abcam).

Glutamate dose-response effect

Müller glial cells (8×10^3) were seeded onto 96-well plate for 48 h in appropriate culture medium. Then, cells were incubated with increased glutamate concentrations (0, 0.1, 1 and 10 mM) in FBS-free DMEM-F12 culture medium and cell viability was assessed using the Prestoblue Reagent (Life technologies).

Quantification of apoptosis (TUNEL technology)

In vivo detection of individual apoptotic cells was done in frozen and formalin-fixed retinal sections of *Opa1* mice using the *In Situ* Cell Death Detection Kit, TMR red (Roche Diagnostics). The same experiment was applied to primary cultures of *Opa1*^{delTTAG} Müller glial cells. Cells were seeded on a 24-well plate (20 000 cells/well) and cultivated with appropriate culture medium for 48 h. TUNEL labelling was done on formalin-fixed cells. Retinal and cell samples were then analyzed under a fluorescence microscope (Confocal Zeiss LSM510 META) and positive cells were counted. Co-immuno labelling with the Brn3a antibody was done to identify RGC nuclei.

OPA1 patient cohorts

One hundred and sixty-one ADOA patients with confirmed *OPA1* mutation were retrospectively analysed from three centres: 1/the centre for sensorineural diseases, Gui de Chauliac Hospital, Montpellier, France (71 patients), 2/the Ophthalmology Department, Glostrup University Hospital, Copenhagen and the National Eye Clinic, Kennedy Centre, Glostrup, Denmark (68 patients) and 3/the Department of Ophthalmology, University Hospital Angers, France (15 patients). We considered visual acuity measurement on Snellen or Monoyer charts, which was subsequently transformed in LogMAR units for statistical purposes, and RNFL measurements using a Heidelberg Retinal Tomograph (HRT-II, software version 2.0, Heidelberg Engineering GmbH, Heidelberg, Germany) on patients from Montpellier and using HD-OCT (Cirrus, software version 6.0, Carl Zeiss Meditec, Dublin, CA) on patients from Denmark and Angers.

Statistical analysis

Mann-Withney U-test and one-way ANOVA followed by the Student-Newman-Keuls multiple comparison test were used when appropriated. Statistical significance thresholds were determined at $P < 0.05$ (*), $P < 0.01$ (**) and $P < 0.001$ (***) values.

Study approval

All protocols carried out on animals were approved by the Animal Care and Use Committee Languedoc-Roussillon and recorded under the reference: CEEA-LR-11058, in agreement with the ARRIVE guidelines. All efforts were made to minimize the number of used animals and their suffering, according to the European directive 2010/63/UE. The authors confirm that they are in compliance with their Institutional Review Boards. The

Department of Ophthalmology of the Hospital of Montpellier has the authorization no. 11018S from the French Ministry of Health for biomedical research in the field of physiology, pathophysiology, epidemiology and genetics in ophthalmology.

Acknowledgements

The authors gratefully acknowledge Dr J-P Hugnot for Sox2 antibody, Dr R Nouvian for glutamate supply, Dr P Brabet and M Teigell for their technical expertise as well as Dr H Boukhaddaoui for microscopy image analysis (MRI plateform). We also thank Dr Françoise Paris for advices in Endocrinology, Dr P Carroll and Dr W Le Goff for critical reading of the manuscript.

Conflict of Interest statement. None declared.

Funding

This work was supported by the Fondation pour la Recherche Médicale, Retina France, Information Recherche Rétinite Pigmentaire and UNADEV associations, Inserm and University of Montpellier.

References

1. Lenaers, G., Hamel, C., Delettre, C., Amati-Bonneau, P., Procaccio, V., Bonneau, D., Reynier, P. and Milea, D. (2012) Dominant optic atrophy. *Orphanet J. Rare Dis.*, **7**, 46.
2. Elachouri, G., Vidoni, S., Zanna, C., Pattyn, A., Boukhaddaoui, H., Gaget, K., Yu-Wai-Man, P., Gasparre, G., Sarzi, E., Delettre, C. *et al.* (2011) OPA1 links human mitochondrial genome maintenance to mtDNA replication and distribution. *Genome Res.*, **21**, 12–20.
3. Olichon, A., Baricault, L, Gas, N., Guillou, E., Valette, A., Belenguer, P. and Lenaers, G. (2003) Loss of OPA1 perturbates the mitochondrial inner membrane structure and integrity, leading to cytochrome c release and apoptosis. *J. Biol. Chem.*, **278**, 7743–7746.
4. Olichon, A., Guillou, E., Delettre, C., Landes, T., Arnauné-Pelloquin, L., Emorine, L.J., Mils, V., Daloyau, M., Hamel, C., Amati-Bonneau, P. *et al.* (2006) Mitochondrial dynamics and disease, OPA1. *Biochim. Biophys. Acta*, **1763**, 500–509.
5. Amati-Bonneau, P., Milea, D., Bonneau, D., Chevrollier, A., Ferré, M., Guillet, V., Gueguen, N., Loiseau, D., de Crescenzo, M.A., Verny, C. *et al.* (2009) OPA1-associated disorders: phenotypes and pathophysiology. *Int. J. Biochem. Cell Biol.*, **41**, 1855–1865.
6. Leruez, S., Milea, D., Defoort-Dhellemmes, S., Colin, E., Crochet, M., Procaccio, V., Ferré, M., Lamblin, J., Drouin, V., Vincent-Delorme, C. *et al.* (2013) Sensorineural hearing loss in OPA1-linked disorders. *Brain*, **136(Pt 7)**, e236.
7. Yu-Wai-Man, P., Griffiths, P.G., Gorman, G.S., Lourenco, C.M., Wright, A.F., Auer-Grumbach, M., Toscano, A., Musumeci, O., Valentino, M.L., Caporali, L. *et al.* (2010) Multi-system neurological disease is common in patients with OPA1 mutations. *Brain*, **133(Pt 3)**, 771–786.
8. Carelli, V., Musumeci, O., Caporali, L., Zanna, C., La Morgia, C., Del Dotto, V., Porcelli, A.M., Rugolo, M., Valentino, M.L., Iommarini, L. *et al.* (2015) Syndromic parkinsonism and dementia associated with OPA1 missense mutations. *Ann. Neurol.*, **78**, 21–38.
9. Sarzi, E., Angebault, C., Seveno, M., Gueguen, N., Chaix, B., Bielicki, G., Boddaert, N., Mausset-Bonnefont, A.L., Cazevieille, C., Rigau, V. *et al.* (2012) The human OPA1delTTAG mutation induces premature age-related systemic neurodegeneration in mouse. *Brain*, **135(Pt 12)**, 3599–3613.
10. Cohn, A.C., Toomes, C., Hewitt, A.W., Kearns, L.S., Inglehearn, C.F., Craig, J.E. and Mackey, D.A. (2008) The natural history of OPA1-related autosomal dominant optic atrophy. *Br. J. Ophthalmol.*, **92**, 1333–1336.
11. Gaignard, P., Savouroux, S., Liere, P., Pianos, A., Thérond, P., Schumacher, M., Slama, A. and Guennoun, R. (2015) Effect of sex differences on brain mitochondrial function and its suppression by ovariectomy and in aged mice. *Endocrinology*, en20141913.
12. Giordano, C., Montopoli, M., Perli, E., Orlandi, M., Fantin, M., Ross-Cisneros, F.N., Caparrotta, L., Martinuzzi, A., Ragazzi, E., Ghelli, A. *et al.* (2011) Oestrogens ameliorate mitochondrial dysfunction in Leber's hereditary optic neuropathy. *Brain*, **134(Pt 1)**, 220–234.
13. Guarneri, P., Cascio, C., Russo, D., D'Agostino, S., Drago, G., Galizzi, G., De Leo, G., Piccoli, F., Guarneri, M. and Guarneri, R. (2003) Neurosteroids in the retina: neurodegenerative and neuroprotective agents in retinal degeneration. *Ann. N. Y. Acad. Sci.*, **1007**, 117–128.
14. Miller, W.L. (2013) Steroid hormone synthesis in mitochondria. *Mol. Cell. Endocrinol.*, **379**, 62–73.
15. Sandoval, H., Yao, C.K., Chen, K., Jaiswal, M., Donti, T., Lin, Y.Q., Bayat, V., Xiong, B., Zhang, K., David, G. *et al.* (2014) Mitochondrial fusion but not fission regulates larval growth and synaptic development through steroid hormone production. *eLife*, **3**.
16. Rone, M.B., Midzak, AS., Issop, L., Rammouz, G., Jagannathan, S., Fan, J., Ye, X., Blonder, J., Veenstra, T. and Papadopoulos, V. (2012) Identification of a dynamic mitochondrial protein complex driving cholesterol import, trafficking, and metabolism to steroid hormones. *Mol. Endocrinol.*, **26**, 1868–1882.
17. Wasilewski, M., Semenzato, M., Rafelski, S.M., Robbins, J., Bakardjiev, A.I. and Scorrano, L. (2012) Optic atrophy 1-dependent mitochondrial remodeling controls steroidogenesis in trophoblasts. *Curr. Biol.*, **22**, 1228–1234.
18. Puomila, A., Huoponen, K., Mäntyjärvi, M., Hämäläinen, P., Paananen, R., Sankila, E.M., Savontaus, M.L., Somer, M. and Nikoskelainen, E. (2005) Dominant optic atrophy: correlation between clinical and molecular genetic studies. *Acta Ophthalmol. Scand.*, **83**, 337–346.
19. Votruba, M., Fitzke, F.W., Holder, G.E., Carter, A., Bhattacharya, S.S. and Moore, A.T. (1998) Clinical features in affected individuals from 21 pedigrees with dominant optic atrophy. *Arch. Ophthalmol.*, **116**, 351–358.
20. Ronnback, C., Milea, D. and Larsen, M. (2013) Imaging of the macula indicates early completion of structural deficit in autosomal-dominant optic atrophy. *Ophthalmology*, **120**, 2672–2677.
21. Pierron, D., Ferré, M., Rocher, C., Chevrollier, A., Murail, P., Thoraval, D., Amati-Bonneau, P., Reynier, P. and Letellier, T. (2009) OPA1-related dominant optic atrophy is not strongly influenced by mitochondrial DNA background. *BMC Med. Genet.*, **10**, 70.
22. Guarneri, P., Guarneri, R., Cascio, C., Pavasant, P., Piccoli, F. and Papadopoulos, V. (1994) Neurosteroidogenesis in rat retinas. *J. Neurochem.*, **63**, 86–96.
23. Reddy, D.S. (2010) Neurosteroids: endogenous role in the human brain and therapeutic potentials. *Prog. Brain Res.*, **186**, 113–137.

24. Vallée, M., Vitiello, S., Bellocchio, L., Hébert-Chatelain, E., Monlezun, S., Martin-Garcia, E., Kasanetz, F., Baillie, G.L., Panin, F., Cathala, A. *et al.* (2014) Pregnenolone can protect the brain from cannabis intoxication. *Science*, **343**, 94–98.
25. Cascio, C., Russo, D., Drago, G., Galizzi, G., Passantino, R., Guarneri, R. and Guarneri, P. (2007) 17beta-estradiol synthesis in the adult male rat retina. *Exp. Eye Res.*, **85**, 166–172.
26. Zheng, W., Reem, R.E., Omarova, S., Huang, S., DiPatre, P.L., Charvet, C.D., Curcio, C.A. and Pikuleva, I.A. (2012) Spatial distribution of the pathways of cholesterol homeostasis in human retina. *PloS One*, **7**, e37926.
27. Lemmen, J.G., van den Brink, C.E., Legler, J., van der Saag, P.T. and van der Burg, B. (2002) Detection of oestrogenic activity of steroids present during mammalian gestation using oestrogen receptor alpha- and oestrogen receptor beta-specific in vitro assays. *J. Endocrinol.*, **174**, 435–446.
28. Ihionkhan, C.E., Chambliss, K.L., Gibson, L.L., Hahner, L.D., Mendelsohn, M.E. and Shaul, P.W. (2002) Estrogen causes dynamic alterations in endothelial estrogen receptor expression. *Circ. Res.*, **91**, 814–820.
29. Ishunina, T.A., Kruijver, F.P., Balesar, R. and Swaab, D.F. (2000) Differential expression of estrogen receptor alpha and beta immunoreactivity in the human supraoptic nucleus in relation to sex and aging. *J. Clin. Endocrinol. Metab.*, **85**, 3283–3291.
30. Pillai, S.B., Jones, J.M. and Koos, R.D. (2002) Treatment of rats with 17beta-estradiol or relaxin rapidly inhibits uterine estrogen receptor beta1 and beta2 messenger ribonucleic acid levels. *Biol. Reprod.*, **67**, 1919–1926.
31. Shima, N., Yamaguchi, Y. and Yuri, K. (2003) Distribution of estrogen receptor beta mRNA-containing cells in ovariectomized and estrogen-treated female rat brain. *Anat. Sci. Int.*, **78**, 85–97.
32. Yang, S.H., Liu, R., Perez, E.J., Wen, Y., Stevens, S.M., Jr., Valencia, T., Brun-Zinkernagel, A.M., Prokai, L., Will, Y., Dykens, J., Koulen, P. and Simpkins, J.W. (2004) Mitochondrial localization of estrogen receptor beta. *Proc. Natl. Acad. Sci. USA*, **101**, 4130–4135.
33. Rettberg, J.R., Yao, J. and Brinton, R.D. (2014) Estrogen: a master regulator of bioenergetic systems in the brain and body. *Front. Neuroendocrinol.*, **35**, 8–30.
34. Long, J., He, P., Shen, Y. and Li, R. (2012) New evidence of mitochondria dysfunction in the female Alzheimer's disease brain: deficiency of estrogen receptor-beta. *Journal of Alzheimer's Disease: JAD*, **30**, 545–558.
35. Bringmann, A., Pannicke, T., Grosche, J., Francke, M., Wiedemann, P., Skatchkov, S.N., Osborne, N.N. and Reichenbach, A. (2006) Muller cells in the healthy and diseased retina. *Prog. Retin. Eye Res.*, **25**, 397–424.
36. Cascio, C., Guarneri, R., Russo, D., De Leo, G., Guarneri, M., Piccoli, F. and Guarneri, P. (2000) Pregnenolone sulfate, a naturally occurring excitotoxin involved in delayed retinal cell death. *J. Neurochem.*, **74**, 2380–2391.
37. Cascio, C., Guarneri, R., Russo, D., De Leo, G., Guarneri, M., Piccoli, F. and Guarneri, P. (2002) A caspase-3-dependent pathway is predominantly activated by the excitotoxin pregnenolone sulfate and requires early and late cytochrome c release and cell-specific caspase-2 activation in the retinal cell death. *J. Neurochem.*, **83**, 1358–1371.
38. Guarneri, P., Russo, D., Cascio, C., De Leo, G., Piccoli, F. and Guarneri, R. (1998) Induction of neurosteroid synthesis by NMDA receptors in isolated rat retina: a potential early event in excitotoxicity. *Eur. J. Neurosci.*, **10**, 1752–1763.
39. Hill, M., Lukác, D., Lapcík, O., Sulcová, J., Hampl, R., Pouzar, V. and Stárka, L. (1999) Age relationships and sex differences in serum levels of pregnenolone and 17-hydroxypregnenolone in healthy subjects. *Clin. Chem. Lab. Med.* **37**, 439–447.
40. Watzka, M., Bidlingmaier, F., Schramm, J., Klingmuller, D. and Stoffel-Wagner, B. (1999) Sex- and age-specific differences in human brain CYP11A1 mRNA expression. *J. Neuroendocrinol.*, **11**, 901–905.
41. Chekroud, K., Arndt, C., Basset, D., Hamel, C.P., Brabet, P. and Pequignot, M.O. (2011) Simple and efficient: validation of a cotton wick electrode for animal electroretinography. *Ophthalm. Res.*, **45**, 174–179.
42. Prusky, G.T., Alam, N.M., Beekman, S. and Douglas, R.M. (2004) Rapid quantification of adult and developing mouse spatial vision using a virtual optomotor system. *Invest. Ophthalmol. Vis. Sci.*, **45**, 4611–4616.
43. Medja, F., Allouche, S., Frachon, P., Jardel, C., Malgat, M., Mousson de Camaret, B., Slama, A., Lunardi, J., Mazat, J.P. and Lombès, A. (2009) Development and implementation of standardized respiratory chain spectrophotometric assays for clinical diagnosis. *Mitochondrion*, **9**, 331–339.